tions yields crystallites that coherently span the entire thickness of the film. However, the (311) layers are apparently stacked with fewer defects during growth than the other planes, even though the CaF_2 (111) substrate was chosen to provide a lattice-matched template for the close-packed planes of C_{60} (*3*). The preference for (311) planes in the films could be because they are thermodynamically more stable or they are kinetically favored and simply grow faster than the other orientations.

The rolling hillock morphology revealed in Fig. 2 resembles that of amorphous surfaces, such as those formed by the sputtering of graphite (*13*), rather than the faceted surface of a polycrystalline film. The kinetics of the formation of hillocks has been explained in terms of the competition between the stochastic arrival of deposited particles, which leads to a totally random structure, and the diffusion of particles on the surface, which leads to correlation of the features on the surface (*13, 14*). For the extremely low deposition rates of the C_{60} films grown for this study, the morphology of the films should be determined primarily by surface diffusion. Since room temperature represents a very high temperature for the weakly bonded C_{60} molecules, the exposed surfaces should be close to thermodynamic equilibrium structures.

A thermodynamically stable (311) orientation for the exposed surface is completely counterintuitive. The lowest energy surface for an fcc solid should be a (111) plane, whereas the (311) is normally a relatively high energy surface (*15*). We propose that the fcc (311) surface of solid C_{60} is stabilized relative to the (111) close-packed surface at room temperature because of the higher entropy afforded by the more open surface. With its large moment of inertia and spherical shape, C_{60} rotates in its bulk crystal lattice sites down to at least 100 K (*16*). The row separations in the (311) surface reduce the number of nearest neighbors in the surface plane from six to two compared to a close-packed surface and thus may allow less hindered rotations of the molecules at the surface. In addition, a more open structure allows more disorder in the rows, as observed in Fig. 3, A and B. This entropy gain could lower the surface free energy of the (311) plane relative to the close-packed surface and thus stabilize the (311) surface at room temperature.

Since the forces among C_{60} molecules are primarily van der Waals in nature, there is a great temptation to regard the solid as a noble gas ice in which the individual "atoms" have a mass of 720 AMU. Indeed, solid Ne, Ar, Kr, and Xe all have the fcc structure, and solid C_{60} appears to continue that trend. However, the large number of internal degrees of freedom in C_{60} makes any intuition based upon the packing of atoms in a crystal lattice tenuous at best. The fact that the free surfaces of our C_{60} films have an open (311) structure that is stable with respect to scanning with an AFM tip may be a manifestation of the internal structure of these nominally spherical molecules and the role that entropy plays in stacking the molecules.

REFERENCES AND NOTES

1. W. Krätschmer, L. D. Lamb, K. Fostiropoulos, D. R. Huffman, *Nature* **347**, 354 (1990).
2. H. Ajie *et al.*, *J. Phys. Chem.* **94**, 8630 (1990).
3. W. M. Tong *et al.*, *ibid.*, **95**, 4709 (1991).
4. J. L. Wragg, J. E. Chamberlain, H. W. White, W. Krätschmer, D. R. Huffman, *Nature* **348**, 623 (1990).
5. R. J. Wilson *et al.*, *ibid.*, p. 621.
6. Y. Z. Li *et al.*, *Science* **252**, 547 (1991).
7. A. Guinier, *X-Ray Diffraction* (Freeman, San Francisco, 1963), pp. 121–125.
8. T. R. Albrecht and C. F. Quate, *J. Vac. Sci. Technol* **A6**, 271 (1988).
9. J. F. Nicholas, *An Atlas of Models of Crystal Surfaces* (Gordon and Breach, New York, 1965).
10. R. M. Fleming *et al.*, *Mat. Res. Soc. Proc.*, in press.
11. P. A. Heiney *et al.*, *Phys. Rev. Lett.* **66**, 2911, (1991).
12. J. E. Fischer *et al.*, *Science* **252**, 547 (1991).
13. E. A. Eklund, R. Briunsma, J. Rudnick, R. S. Williams, in preparation.
14. G. S. Bales *et al.*, *Science* **249**, 264, (1990).
15. A. Zangwill, *Physics at Surfaces* (University Press, Cambridge, 1988), p. 14.
16. C. S. Yannoni, R. D. Johnson, G. Meijer, D. S. Bethune, J. R. Salem, *J. Phys. Chem.* **95**, 9 (1991).

17. This work was supported in part by the Office of Naval Research (E.J.S., W.M.T., and R.S.W.) and the National Science Foundation (S.J.A., M.M.A., Y.R., F.N.D., and R.L.W.). Some of the work described in this paper was carried out at the Jet Propulsion Laboratory, California Institute of Technology through an agreement with the National Aeronautical and Space Administration.

29 April 1991; accepted 10 June 1991

Field-Induced Nanometer- to Atomic-Scale Manipulation of Silicon Surfaces with the STM

IN-WHAN LYO AND PHAEDON AVOURIS

The controlled manipulation of silicon at the nanometer scale will facilitate the fabrication of new types of electronic devices. The scanning tunneling microscope (STM) can be used to manipulate strongly bound silicon atoms or clusters at room temperature. Specifically, by using a combination of electrostatic and chemical forces, surface atoms can be removed and deposited on the STM tip. The tip can then move to a predetermined surface site, and the atom or cluster can be redeposited. The magnitude of such forces and the amount of material removed can be controlled by applying voltage pulses at different tip-surface separations.

THERE HAS BEEN A CONTINUING EFFORT to find ways to manipulate materials at ever decreasing length scales. The ability of the STM to address and probe individual surface sites makes it a promising tool for the manipulation of materials on the nanometer scale (*1*). In particular, soon after the development of the STM (*2*) the possibility of transferring material between the tip and the sample was discussed (*3*). Early work established that voltage pulses applied to the STM tip can lead to the deposition of material on the sample surface (*4, 5*), while in other cases (*6, 7*) pits were created on the surface. The early work was exploratory, and the mechanisms by which the surface modifications took place were not established. However, in two recent STM studies involving desorption of adsorbates from silicon (*8*) and deposition of gold particles from a god tip (*9*), the strong electric fields that can develop between the tip and the sample were invoked. Similarly, the field enhancement of adsorbate diffusion processes (*8, 10*) was suggested.

We show that even the strongly and covalently bonded silicon substrate atoms can be manipulated with the STM, and we analyze the mechanisms by which this is accomplished. Specifically, by combining the effects of the strong electric field formed between the STM tip and the surface with chemical tip-sample interactions, we reproducibly transfer Si atoms and Si clusters up to tens of atoms from the surface to the tip. Moreover, we could then redeposit these clusters or atoms at predetermined sites of the surface. The mechanism involves a field-evaporation process with a low-threshold field that is modified by chemical and mechanical tip-sample interactions. The STM used in these studies as well as of the techniques used in sample preparation have been described previously (*11*).

Field evaporation involves the ionization and desorption of individual atoms or clus-

IBM Research Division, T. J. Watson Research Center, Yorktown Heights, NY 10598.

ters of atoms from the surface of a material by the application of a strong electric field (*12*). The material is usually in the form of a sharp tip, as in field ion microscopy (FIM) (*12*). In the STM, large electric fields can develop between the tip and the surface sites directly below it. In this configuration one can vary the field intensity either by applying variable voltage pulses at a fixed tip-sample separation or by applying the same voltage pulse but varying the tip-sample distance. At small tip-sample separations the field effect is supplemented by chemical tip-sample interactions. In order to control the spatial extent of the region affected by field evaporation, we varied the tip-sample distance. As a measure of the chemical tip-sample interaction we used the effective tunneling barrier ϕ_{eff}, which is defined by $I_{tun} = V \exp[-1.025s\ (\phi_{eff})^{1/2}]$, where I_{tun} is the tunneling current, V is the applied voltage, s is the tip-sample distance (given in angstroms), and ϕ_{eff} is given in electron volts (*13*). Experiments (*14*) and calculations (*15, 16*) on metal surfaces have shown that as the tip-sample distance decreases ϕ_{eff} is reduced and eventually ϕ_{eff} collapses to zero. In Fig. 1 we show ϕ_{eff} as a function of the z-piezoelectric displacement for the Si(111)-(7 × 7)–W tip system. It is seen that ϕ_{eff} collapses to zero within a region of only ~3 Å. The fields and chemical forces acting on the surface atoms in this region are very strong. If we define the electronic contact point at which ϕ_{eff} collapses as the zero in the tip-sample separation scale, we find that under normal tunneling conditions (V_{bias} = +2 V and I_{tun} = 200 pA) the tip-sample distance is ~6 Å. In order to induce field evaporation we typically moved the tip from this normal position toward the surface by a predetermined distance with no bias voltage applied. At the closest point, a 10-ms voltage pulse was applied and the tip was then retracted back to its normal position and the surface was imaged again. In order to better understand the nature of the tip-surface interaction, an alternative approach was also used. In this case, as the tip approached the surface, the bias voltage was ramped and I-V curves as a function of tip-sample distance were thus obtained.

The various surface structures that could be generated by applying voltage pulses to the sample (+3 V in all cases), along with their probability of formation as a function of tip displacement, are shown in Fig. 2. In Fig. 2A the voltage pulse was applied after the tip was moved 3 Å toward the sample, while in Fig. 2, B and C, the tip was moved by 4 and 5 Å, respectively. As the field was gradually increased, the first type of structure that appeared at a threshold field of ~1 V/Å was a small mound, such as that of Fig. 2A. As the field was increased further by increasing the tip displacement, we typically observed the clean removal of the first Si atom layer. Such a structure with a diameter of ~40 Å is shown in Fig. 2B. In order to create smaller features, the tip has to approach closer to the surface and a weaker pulse must be applied. As Fig. 2D shows, even removal of a single Si atom is possible (tip displacement 5 Å and pulse +1 V). Single atom desorption is, however, less reproducible than cluster desorption because it critically depends on the sharpness of the tip.

At shorter tip-sample distances the dominant structure involves a mound surrounded by a moat (Fig. 2C). It is likely that this structure is formed when desorbing Si atoms are pulled and pile up under the apex of the tip, which is the point of the maximum field strength. The mound in fact forms a bridge that connects the sample and the tip. This is supported by the results in Fig. 3, which shows the variation of the current with tip-sample separation. Initially the cur-

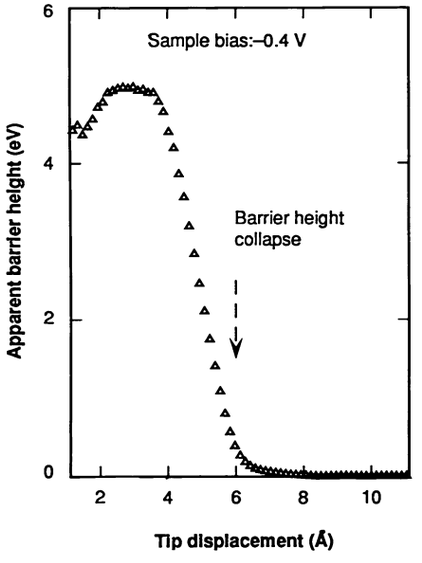

Fig. 1. Apparent tunneling barrier height as a function of the tip displacement toward the surface. The displacement is measured from the tip position at which the tunneling current is 200 pA at +2-V bias (normal tunneling conditions).

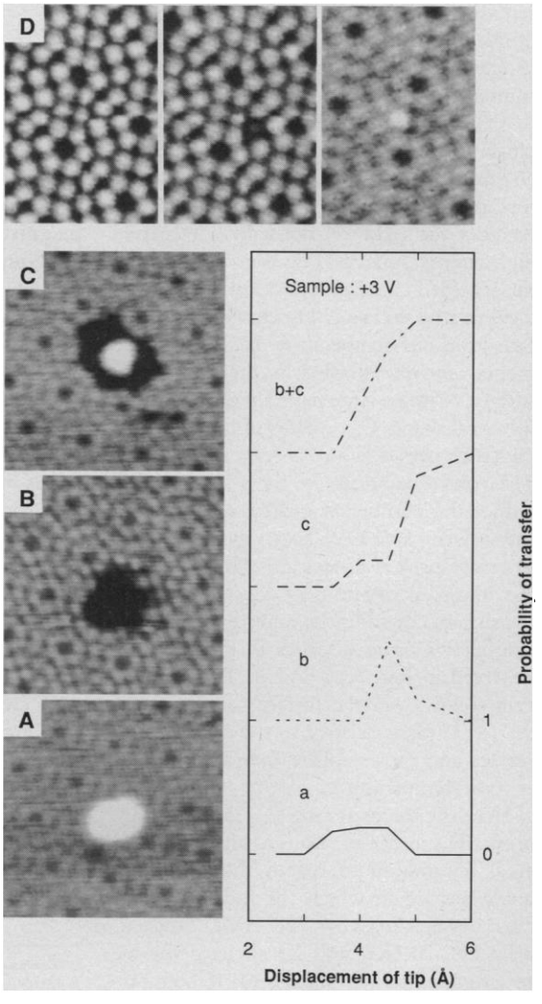

Fig. 2. (**A** to **C**) Typical surface structures created by the application of a +3-V pulse to the sample. Also shown are the corresponding probabilities of forming such structures as a function of tip displacement. (**D**) Removal of a single Si atom. From left to right the images are taken before and after the voltage pulse (+1 V and tip displacement of 5 Å) was applied and, finally, after the redeposition of the atom back to the surface.

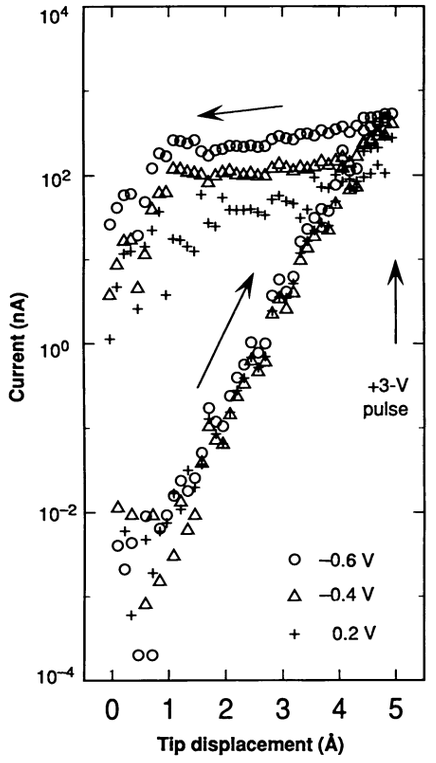

Fig. 3. Tunneling current versus tip displacement. The tip was first displaced toward the surface and, after a pulse was applied at the point indicated by the arrow, it was retracted away from the surface. The resulting surface structure is similar to that shown in Fig. 2C.

rent varies exponentially with decreasing tip-sample separation. At the point indicated by the arrow the voltage pulse was applied. After the pulse the tip was retracted but only a weak dependence of the current on the z-piezo voltage was observed; this corresponded to the stretching of the bridge formed between tip and sample. Finally, at a nominal tip retraction of 4 Å the bridge was broken and again the current dropped off exponentially. Most likely the simple raised mound typified by Fig. 2A was also formed by desorbing Si atoms that had not quite escaped the influence of the surface. If such a mound is pulsed again it is usually cleanly removed and leaves behind a hole, such as that shown in Fig. 2B. In general, we have found that the features produced by a voltage pulse can be modified or even eliminated by subsequent pulses (see below). As Fig. 2 shows, the lower bound for the threshold field for desorption is ~1 V/Å. This threshold field is significantly lower than the threshold fields of 3.0 to 3.8 V/Å reported in FIM studies (*12*).

The STM can be used not only to remove Si atoms, but as Fig. 4 shows, it can also be used to deposit them anywhere on the surface. In Fig. 4A we show again the topograph of a typical mound and moat structure. We placed the tip over the mound and applied a second + 3-V pulse to the sample. This second pulse removed cleanly the entire mound and transferred the Si cluster to the tip. The tip carrying the Si cluster was then moved to the left side of the hole, and the cluster was redeposited to the surface by applying a voltage pulse of the opposite polarity (−3 V). In Fig. 4, C and D, we show the corresponding line scans. Single-atom deposition is shown in the right-most panel of Fig. 2D. We found that the desorption of Si clusters from the tip by applying voltage pulses to the sample is a very reproducible process. When the Si on the tip is exhausted, the desorption stops. We find no evidence for desorption of tip material under the conditions that Si is desorbed. In this respect we note that desorption of W from the W tip should require 2 V/Å greater threshold fields (*12*).

We have also examined to what extent mechanical tip-sample interactions may contribute to the surface modifications reported here. We have tested this by driving the tip to the surface without an applied bias. We found that modifications do take place but that they require nominal tip displacements greater than those involved in our experiments (that is, direct tip-surface contact). The topographies of the resulting surface modifications (protrusions) are similar to those of Fig. 2A. Another possibility involves thermal effects. However, the dimensions of the modified areas (1 to 5 nm) are too small compared with the thermal diffusion length in the Si sample (~10 μm), so it is unlikely that thermal effects play a dominant role (*17*).

All of the available evidence, that is, the existence of a threshold, the reversibility of the transfer of material, and the nature of the induced modifications, point to an electronic mechanism in general, and to a field-evaporation mechanism in particular. The threshold field we find is, however, significantly lower than that observed in FIM studies. At relatively large tip-sample separations the simultaneous image-like interaction of the desorbing ion with both surface and tip should decrease the threshold field to a value lower than that in FIM (*8, 9*). As this distance is further reduced, classical image effects do not provide a proper description of the interactions involved, which are in this case dominated by chemical effects. These chemical effects should strongly reduce the threshold field. Another factor that should be considered is the large current density generated by the voltage pulse and its possible role in softening the strength of chemical bonding. Finally, although field evaporation may be the mechanism by which the desorption process is initiated, more complex processes are likely to contribute in the later stages of the process. As we discussed above, mounds formed by the desorbed Si atoms bridge the gap and connect the tip and substrate. It is clear that high fields and currents are created in the process and that mechanical effects induced during the retraction of the tip can affect the final morphology.

The advantage of the STM for removing and depositing Si atoms is that these processes can be induced in preselected areas. The close proximity of tip and sample in the STM configuration leads to threshold fields, ~1 V/Å in the case of Si, that are lower than those deduced from previous FIM studies. The field-induced processes discussed here provide a powerful tool for the nanometer-scale processing of strongly bound materials and could find a variety of applications, such as building nanometer-scale Si and other semiconductor structures, producing and depositing clusters for study by scanning tunneling spectroscopy and other techniques, or generating local doping schemes. These capabilities may thereby enable an entirely new era of semiconductor micro-

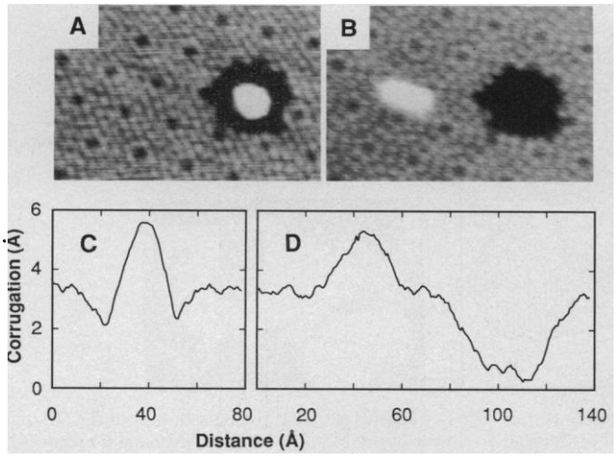

Fig. 4. In (**A**), a +3-V pulse has led to the formation of a typical mound and moat structure. In (**B**), a second +3-V pulse was applied to remove the Si mound. The tip was then moved to the left and, by applying a −3-V pulse, the Si cluster on the tip was deposited on the surface. Line scans across the structures shown in (A) and (B) are given in (**C**) and (**D**), respectively.

electronics, which we refer to as "nanoelectronics."

REFERENCES AND NOTES

1. For reviews, see: C. F. Quate, in *Highlights of the 80's and Prospects for the 90's in Condensed Matter Physics*, L. Esaki, Ed. (Plenum, New York, 1991); G. M. Shedd and P. E. Russel, *Nanotechnology* **1**, 67 (1990).
2. G. Binnig, H. Rohrer, Ch. Gerber, E. Weibel, *Phys. Rev. Lett.* **49**, 59 (1982).
3. R. Gomer, *IBM J. Res. Dev.* **30**, 428 (1986).
4. R. S. Becker, J. A. Golovchenko, B. S. Swartzentrouber, *Nature* **325**, 419 (1987).
5. J. S. Foster, J. E. Frommer, P. C. Arnett, *ibid.* **331**, 324 (1988).
6. R. Emch, J. Nogami, M. M. Dovek, C. A. Lang, C. F. Quate, *J. Microsc.* **152**, 129 (1988).
7. Y. Z. Li, L. Vazquez, R. Piner, R. P. Andres, R. Reifenberger, *Appl. Phys. Lett.* **54**, 1424 (1989).
8. I.-W. Lyo and Ph. Avouris, *J. Chem. Phys.* **93**, 4479 (1990).
9. H. M. Mamin, P. H. Guether, D. Rugar, *Phys. Rev. Lett.* **65**, 2418 (1990).
10. L. J. Whitman, J. A. Stroscio, R. A. Dragoset, R. J. Celotta, *Science* **251**, 1206 (1991).
11. Ph. Avouris and R. Wolkow, *Phys. Rev. B* **39**, 509 (1989).
12. T. T. Tsong, *Atom-Probe Field Ion Microscopy* (Cambridge Univ. Press, Cambridge, 1990), and references therein.
13. G. Binnig and H. Rohrer, *Surf Sci.* **126**, 236 (1983).
14. J. K. Gimzewski and R. Möller, *Phys. Rev. B* **36**, 1284 (1987).
15. N. D. Lang, *ibid.* **37**, 10395 (1988).
16. S. Ciraci and E. Tekman, *ibid.* **40**, 11969 (1989).
17. P. F. Marella and R. F. Pease, *Appl. Phys. Lett.* **55**, 2366 (1989).

18. We thank N. Lang for helpful discussions and J. E. Demuth and R. Walkup for a careful reading of the manuscript.

7 May 1991; accepted 13 June 1991

Rapid Eruption of the Siberian Traps Flood Basalts at the Permo-Triassic Boundary

PAUL R. RENNE AND ASISH R. BASU

The Siberian Traps represent one of the most voluminous flood basalt provinces on Earth. Laser-heating $^{40}Ar/^{39}Ar$ data indicate that the bulk of these basalts was erupted over an extremely short time interval (900,000 ± 800,000 years) beginning at about 248 million years ago at mean eruption rates of greater than 1.3 cubic kilometers per year. Such rates are consistent with a mantle plume origin. Magmatism was not associated with significant lithospheric rifting; thus, mantle decompression resulting from rifting was probably not the primary cause of widespread melting. Inception of Siberian Traps volcanism coincided (within uncertainty) with a profound faunal mass extinction at the Permo-Triassic boundary 249 ± 4 million years ago; these data thus leave open the question of a genetic relation between the two events.

AT LEAST 11 DISTINCT EPISODES OF voluminous volcanism have produced flood basalt provinces covering more than 100,000 km^2 in the last 250 million years (*1–3*). The eruption of major flood basalt provinces is generally attributed to the thermal anomaly generated by a subcontinental mantle plume or hot spot (*2, 4–6*). The plume model predicts that initial rapid and voluminous flood basalt eruptions are followed by dimunition of eruption rate and in some cases the production of a hotspot track as a lithospheric plate moves over the mantle plume (*2, 4*).

The paroxysmic effusion of magma and volcanic gases that characterizes initial flood basalt activity may sufficiently disrupt Earth's atmospheric and hydrospheric cycles that biotic crises result (*1, 7, 8*): A celebrated possible example is the eruption of the Deccan Traps, which has been inferred as a mechanism for the Cretaceous-Tertiary faunal mass extinction event (*7*). Comprising roughly 1.5 × 10^6 km^3 of lava, most of the Deccan Traps may have been erupted during a period of less than 1 million years at about 66 Ma (million years ago), coincident within uncertainties with the Cretaceous-Tertiary boundary (*3, 9*). Compelling evidence has also been raised for a meteorite impact at the Cretaceous-Tertiary boundary; this is thought by many to represent a more likely cause for this extinction (*10*).

Some investigators have proposed a relation between major flood basalt events and bolide impacts: Both have been inferred to show a periodicity of 26 to 32 million years that may be in phase and may correlate temporally with periodic faunal mass extinction events (*1*). Uncertainties in the age and duration of many flood basalt provinces, however, inhibit precise temporal correlation between flood basalt episodes, mass extinctions, and bolide impacts.

Arguably the largest Phanerozoic flood basalt province is the Siberian Traps (ST; Fig. 1), which now cover ~3.4 × 10^5 km^2 and which may have had an original volume of >1.5 × 10^6 km^3 (*11–13*). In this report, we present high-precision $^{40}Ar/^{39}Ar$ geochronologic data showing that most of the ST were erupted over a very short time interval (~1 million year) coinciding, within uncertainties, with the Permo-Triassic extinction event that marked the end of the Paleozoic Era.

The ST occur on the northwestern margin of the Siberian Platform where they overlie Carboniferous to Upper Permian lagoonal and terrestrial sedimentary rocks. The flood basalts have a composite thickness greater than 3700 m and include basaltic flows and volumetrically minor basaltic tuffs; significant local variations in thickness apparently reflect basin geometry and the distribution of vents (*12, 14*).

The ST comprise a stratigraphic succession of petrologically distinct suites of flows that are laterally continuous over tens of kilometers. In the Noril'sk region, where at least 45 flows produce the greatest thickness of flows, the ST have been divided into 11 suites (Fig. 2) (*11–13*). Stratigraphic sections elsewhere in the ST can be correlated readily with the Noril'sk section (*13, 15*).

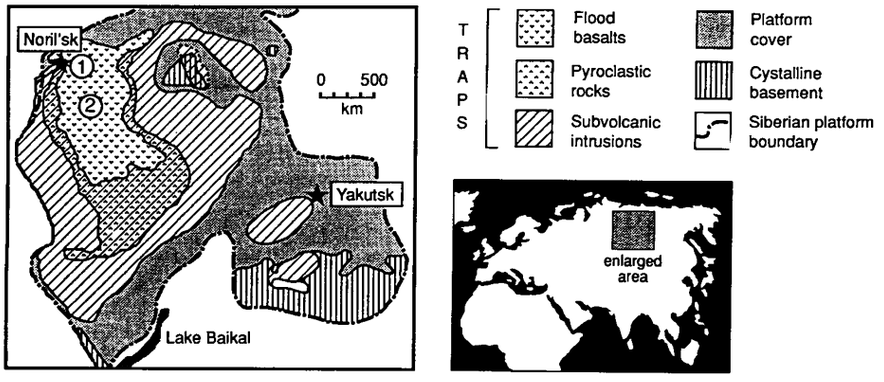

Fig. 1. Geologic sketch map of part of the Siberian platform showing the distribution of the Siberian Traps [after (*11*)]. Circled numbers indicate locations of the Noril'sk (1) and Putorana (2) sections.

P. R. Renne, Institute of Human Origins, Geochronology Center, 2453 Ridge Road, Berkeley, CA 94709.
A. R. Basu, Department of Geological Sciences, University of Rochester, Rochester, NY 14627.